EXPERIMENTAL INVESTIGATIONS OF THE EFFECTS OF CUTTING ANGLE ON CHATTERING OF A FLEXIBLE MANIPULATOR

J. Lew, J. Huggins, D. Magee and W. Book

Flexible Automation Laboratory
George W. Woodruff School of Mechanical Engineering
Georgia Institute of Technology
Atlanta, Georgia 30332

ABSTRACT

When a machine tool is mounted at the tip of a robotic manipulator, the manipulator becomes more flexible (the natural frequencies are lowered). Moreover, for a given flexible manipulator, its compliance will be different depending on feedback gains, configurations, and direction of interest. In this paper, the compliance of a manipulator is derived analytically, and its magnitude is represented as a compliance ellipsoid. Then, using a two link flexible manipulator with an abrasive cut-off saw, the experimental investigation shows that the chattering varies with the saw cutting angle due to the different compliance. The main work is devoted to finding a desirable cutting angle which reduces the chattering.

1. INTRODUCTION

1.1 Motivation

In real world applications, robot manipulators are mechanically very rigid by design. This rigidity is necessary for high positioning accuracy; however, it becomes difficult to perform operations when a rigid manipulator contacts a workpiece. On the other hand, flexible manipulators can provide passive compliance due to their link flexibility. With this structural compliance, certain applications such as cutting a workpiece can be performed with pure position control. Thus, the compliance can provide a simple, inexpensive solution for certain applications that otherwise could not be achieved with position control alone [1,2].

Figure 1 shows the block diagrams of the overall architecture of a cutting process with pure position control. An abrasive cut-off saw is mounted at the tip of a manipulator. Its link flexibility is represented by a spring constant (K_L). The position feedback signal is measured at each joint. Due to the flexibility of the link, it is possible to regulate the force applied to the workpiece by controlling the position of the end-effector relative to the workpiece. However, if the stiffness of the link is high, any uncertainty in the position of the workpiece, or er-

rors in the position servo of the manipulator will induce very large cutting forces. Eventually these uncontrolled large cutting forces will shorten the life of the grinding wheel and the manipulator. Also, the high stiffness (K_L) causes a high frequency oscillationor unstable chattering due to reaction forces from the workpiece. This behavior can be easily explained by a root locus with increasing K_L assuming that the position-controlled robot is a linear mass-damper-spring system. Therefore, the compliance of the manipulator becomes one of the important parameters, and more compliance is desirable in the cutting process with pure position control.

In this paper, the compliance of a manipulator is derived analytically, and its magnitude is represented as a *compliance ellipsoid*. It is shown that the compliance will be different depending on feedback gains, link flexibility, configurations, and direction of interest. Then, using a two link flexible manipulator with an abrasive cut-off saw, the experimental investigation shows that the magnitude of the chattering varies with the saw cutting angle due to the different compliance. The final results show a range of cutting angles with acceptable behavior for a point in the workspace with a near circular compliance ellipsoid.
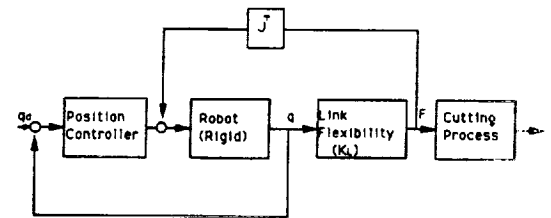

Figure 1. Block Diagram of Cutting Process with a Position-Controlled Manipulator

1.2 Chatter

In the utilization of metal-cutting machine tools, vibrations are often encountered. The contact between the tools and workpiece gives rise to excessive variations of the cutting force which endanger the life of the tool. These vibrations belong to the class of self-excited vibrations. The source of the self-exciting energy is in the cutting process. Furthermore, in many cases, the self-excited vibrations are mixed with forced vibrations excited by various sources such as continuous spinning of the tools [3]. In this paper, the self-excited and forced vibrations are referred to as chatter.

Considerable knowledge about the influence of kinematical parameters on the chatter has been assembled. As yet, however, neither a complete theoretical description and analysis has been accomplished nor reliable ways found for eliminating chatter in grinding [3,4]. By experimental trial and error, general guidelines have been established to reduce the tendency for chatter. Among these are the use of soft-grade wheels, frequent dressing of the wheel, changes in dressing techniques, reduction in material removal rate and more rigid support of the workpiece [8]. Even though many parameters influence the chattering, this paper examines mainly the relationship between the cutting angle and the compliance of the arm.

3. DYNAMIC MODEL

3.1 Cutting Process

Exact modeling of a cutting process can be very complicated [3,4,5,6]. For simplicity, this paper assumes that the cutting forces consist of the normal cutting force which is in the direction of the approach angle of the saw and the tangential cutting force which is perpendicular to the approach angle. The relationship between the normal cutting force (F_n) and tangential cutting force (F_t) can be assumed to be Coulomb friction [7]. i.e.

$$\mu = \frac{F_t}{F_n} = 0.3 \sim 0.4$$

Notice that F_n is larger than F_t. Also, F_t and F_n are a function of the depth of the cut.

3.2 Flexible Manipulator

Modeling a multiple link flexible manipulator is a complicated procedure. The deflection of the arm is approximated as
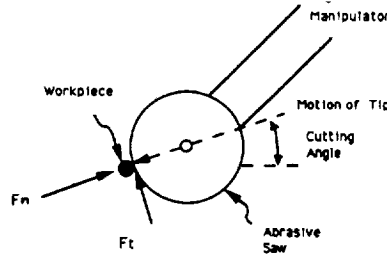

Figure 2. Definition of Cutting Angle

a finite series of separable functions which are the products of mode shape functions $\psi_{ij}(x)$ and time dependent generalized coordinates $q_{fij}(t)$:

$$u_i(x, t) = \sum_{j=1}^{m} \psi_{ij}(x) q_{fij}(t)$$

where i represents the link number and j represents the mode number . The equation of the flexible arm motion can be derived from several techniques, but the Lagrange's formulation is known for its simplicity and systematic approach [9,10]. Using Jacobians to compute the velocity of a point, the kinematic and potential energies are obtained by integrating the velocity and position of the point over the total system. These energies are used in Lagrange's equations. Therefore, the equation of the motion is

$$\begin{bmatrix} M_{rr} & M_{rf} \\ M_{fr} & M_{ff} \end{bmatrix} \begin{pmatrix} \ddot{q}_r \\ \ddot{q}_f \end{pmatrix} + \begin{bmatrix} 0 & 0 \\ 0 & K_L \end{bmatrix} \begin{pmatrix} q_r \\ q_f \end{pmatrix} + \begin{pmatrix} N_r + G_r \\ N_f \end{pmatrix}$$

$$= \begin{bmatrix} I \\ \frac{\partial \psi}{\partial x} \end{bmatrix} T + \begin{bmatrix} J_r^T \\ J_f^T \end{bmatrix} F \qquad (1)$$

where q_r contains the generalized rigid joint coordinates and q_f contains the generalized flexible mode coordinates. M_{ij} is the inertia matrix and K_L represents the link flexibilities . N_r and N_f include nonlinear terms such as the Coriolis and centrifugal force in each coordinate. G_r is the gravity force. T represents joint torques and F represents an end point external force when the contact with environments occurs. Finally, J_r and J_f are the partitions of the Jacobian matrix for a flexible arm.

4. COMPLIANCE OF ARM

The equation of the dynamic motion for a flexible arm is obtained in equation (1). Since the tip of the manipulator proceeds very slowly and in a small range during cutting, the motion can be assumed to be quasi-static and linear. Therefore, the equation of the motion is simplified to the following form assuming the acceleration terms and the velocity terms are negligible.

$$\begin{bmatrix} \frac{\partial G_r}{\partial q_r} \\ 0 \end{bmatrix} \Delta q_r + \begin{bmatrix} 0 & 0 \\ 0 & K \end{bmatrix} \begin{pmatrix} \Delta q_r \\ \Delta q_f \end{pmatrix} = \begin{bmatrix} I \\ \frac{\partial \psi}{\partial x} \end{bmatrix} \tilde{T} + \begin{bmatrix} J_r^T \\ J_f^T \end{bmatrix} F \qquad (2)$$

As shown above in the above equation (2), the gravity force also contributes to a stiffness force. If a joint angle PD controller is applied to the flexible arm, the joint torque $\tilde{T}$ will be

$$\tilde{T} = -K_p \Delta q_r - K_v \Delta \dot{q}_r$$

where K_p and K_v are the feedback gains. This input torque can be interpreted as a spring and a damper force. Again $\dot{q}_r$ can be neglected in quasi-static motion. If we combine all these forces for the stiffness matrix,

2

$$\begin{bmatrix} \frac{\partial G_t}{\partial q} + K_P & 0 \\ 0 & K_L \end{bmatrix} \begin{pmatrix} \Delta q_r \\ \Delta q_f \end{pmatrix} = \begin{bmatrix} J_r^T \\ J_f^T \end{bmatrix} F$$

This stiffness matrix is always invertible. Therefore, it can be rewritten as

$$\begin{pmatrix} \Delta q_r \\ \Delta q_f \end{pmatrix} = \begin{bmatrix} \frac{\partial G_t}{\partial q} + K_P & 0 \\ 0 & K_L \end{bmatrix}^{-1} \begin{bmatrix} J_r^T \\ J_f^T \end{bmatrix} F \qquad (3)$$

Since this matrix shows the relationships between the end-point external force and the joint coordinates, it is necessary to change the joint space to the Cartesian space. Using the Jacobian relationship which is

$$\Delta X = \begin{bmatrix} J_r & J_f \end{bmatrix} \begin{pmatrix} \Delta q_r \\ \Delta q_f \end{pmatrix} \qquad (4)$$

Substituting equation (3) into equation (4) will give

$$\Delta X = \begin{bmatrix} J_r & J_f \end{bmatrix} \begin{bmatrix} \frac{\partial G_t}{\partial q_r} + K_P & 0 \\ 0 & K_L \end{bmatrix}^{-1} \begin{bmatrix} J_r^T \\ J_f^T \end{bmatrix} F \qquad (5)$$

Since compliance is defined as 'displacement per input force', we may say

$$C = \begin{bmatrix} J_r & J_f \end{bmatrix} \begin{bmatrix} \frac{\partial G_t}{\partial q_r} + K_P & 0 \\ 0 & K_L \end{bmatrix}^{-1} \begin{bmatrix} J_r^T \\ J_f^T \end{bmatrix} \qquad (6)$$

This matrix, C, is called the compliance matrix for a flexible arm with a joint angle PD controller. This compliance matrix includes not only link flexibilities, but also feedback gains, stiffness and configurations of the arm. The link flexibilities are represented by K_L and the feedback gains by K_P. The configurations of the arm are represented by J_r and G_r. However, the compliance matrix does not incorporate the mass properties of the arm which also may influence the arm's behavior. If equation (6) is expanded, it can be rewritten as
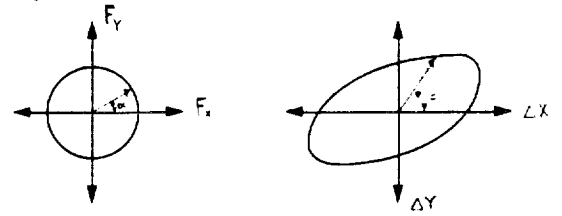
$$C = J_r \left(\frac{\partial G_r}{\partial q_r} + K_P \right)^{-1} J_r^T + J_f K_L^{-1} J_f^T \qquad (7)$$

This form of the compliance matrix shows a major difference between a flexible arm and a rigid arm. In a rigid arm case, K_L is assumed to be very large. Therefore, we may ignore the second term of equation (7) although it is the dominant term in a flexible arm case.

Since the compliance is represented with a matrix for a multiple link manipulator, various input force directions cause different directions and sizes of displacements. This may be explained with a linear algebra concept. From equation (5), we see that the compliance is simply a linear transformation that maps the end-point force F in R^3 into a Cartesian space displacement in R^3. The unit sphere in R^3 defined by

$$F^T F \leq 1$$

is a mapping into an ellipsoid in R^3 defined by

(a) Unit Input Force Sphere   (b) Compliance Ellipsoid

Figure 3. Compliance Ellipsoid

$$\Delta X^T (CC^T)^{-1} \Delta X \leq 1$$

This ellipsoid has principal axes $\lambda_1 e_1, \lambda_2 e_2, \lambda_3 e_3$ where e_i is a unit vector and λ_i is an eigenvalue of (CC^T). We call this the 'compliance ellipsoid'. Therefore, a unit force F in the direction α induces a displacement in the direction β as shown in Figure 3.

5. A CASE STUDY

A large experimental arm designated RALF (Robotic Arm, Large and Flexible) has been constructed and is under computer control. RALF has two degrees of freedom in the vertical plane. The length of each link is about 10 feet. At the tip of RALF, an abrasive cut-off saw is mounted as shown in Figure 4. Using the compliance ellipsoid, we explore the desirable cutting angles for RALF with acceptable chattering behavior.

5.1 Analysis

Based on the actual dynamic parameters of RALF, the dynamic equation is derived in the form of equation (1). Then, actuator dynamics are assumed to be constant gains since their bandwidth is very high compared to the arm dynamics. The actuator gains are included in the feedback gains K_P. The nominal configuration during cutting is the following: the first joint angle is 106.6 degrees, and the second joint angle is 101.8 degrees. The compliance matrix is computed and its magnitude is represented in R^2 with an ellipsoid. Simulation results show that the manipulator's axis of least compliance is at an angle 30 degrees with the horizontal and the axis of greatest compliance is at an angle of 120 degrees in Figure 5(a). Therefore, the 120 degrees cutting angle is desirable to produce the least chattering due to its greater compliance. Different shapes of the compliance ellipsoid can be obtained at different configurations. For example, if the first joint is at 110 degrees and the second joint is at 50 degrees, the compliance ellipsoid can be shown as in Figure 5(b).

5.2 Experiments

To measure the chattering in plane motion, two accelerometers are mounted at the tip of RALF. One accelerometer measures the X direction vibration and the other accelerometer measures the Y direction vibration referenced to the manipulator base coordinates. Experiments use three different cutting angles 0, 40 and 90 degrees. The cutting angles are shown as in Figure 6 and the manipulator follows the given trajectory. Each
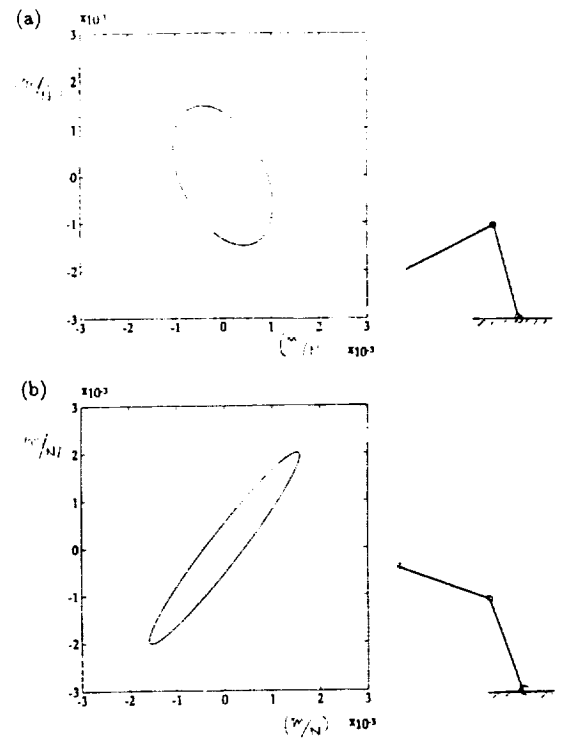
3

Figure 4. RALF with an Abrasive Cut-off Saw

Figure 5. Compliance Ellipsoid for RALF
(a) when $\theta_1 = 106.8$ deg and $\theta_2 = 101.8$ deg
(b) when $\theta_1 = 110$ deg and $\theta_2 = 50$ deg

case assumes that it has the same cutting parameters except for the cutting angle. For instance, cutting velocities are the same for each case, and the same feedback gains are used too. The workpiece is a half inch diameter steel bar and is much stiffer than the manipulator system itself.

First, the abrasive cut-off saw moves very close to the workpiece. Then, the saw is turned on without contact with the workpiece. The vibrational signal is measured by a signal analyzer, and its power spectrum is plotted in Figure 7(a) . The first natural frequency is observed at 4.5 Hz compared to 5 Hz from the mathematical model. Also, another peak is observed at about 62 Hz . This frequency is believed to originate from dynamic imbalance of the saw motor turning at 3800 rpm (63.3 Hz) by the manufacturer's data.

Second, the cut-off saw followed the 0 degree desired trajectory by a joint angle PD control. The trajectory is computed based on Dickerson and Oosting's work [11]. It takes about 10 sec for the saw to go through the workpiece. The acceleration power spectra are measured for 2 sec four times during cutting and are averaged to eliminate the influence of non-periodic noise. The same procedures are used for each experiment. In Figure 7(b), first peak is measured at 9 Hz. We may interpret this shift of the first frequency due to the change in the bound-

ary condition when the saw touches the workpiece. Also, we may notice that the rotation speed of the wheel is reduced due to the contact friction force.

Third, when the saw cuts the workpiece at 40 degrees, the first natural frequency(9 Hz) no longer dominates as before and is mixed with other frequency signals in Figure 7(c). However, the higher mode at 37 Hz becomes more noticeable. In other words, chattering becomes faster.

Fourth, the 90 degree cutting shows smaller magnitudes of vibration in the Y direction , and the mode at 22 Hz becomes important (See Figure 7(d)). We expect that this angle will give the least chattering based on analytical analysis. Experimental
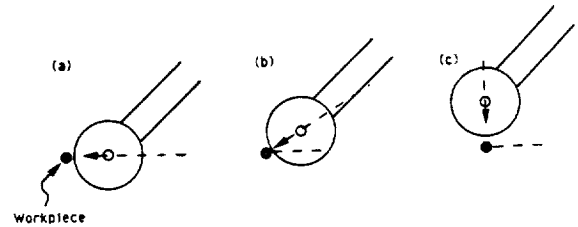

Figure 6. Various Cutting Angle
(a) 0 deg (b) 40 deg (c) 90 deg

4

(a)

Y dir

X dir

(b)

X dir

Y dir
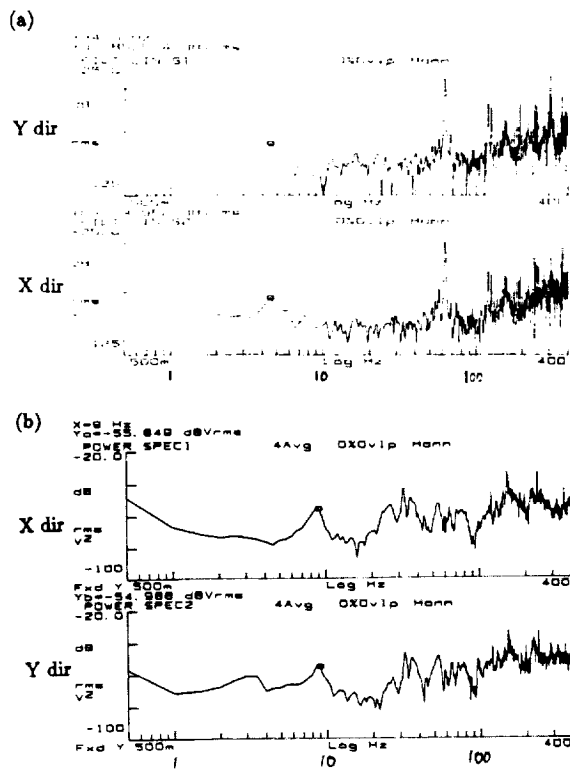
(c)

X dir

Y dir

(d)

X dir

Y dir

Figure 7. Power Spectrum Measurement in X-Y direction
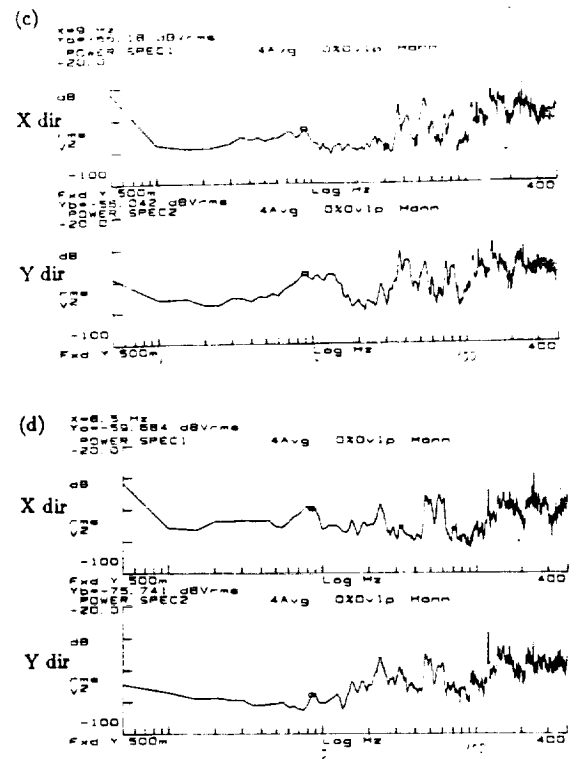(a) Without Any Contact with Workpiece
(b) 0 degrees Cutting Angle

Figure 7. Power Spectrum Measurement in X-Y direction
(c) 40 degrees Cutting Angle
(d) 90 degrees Cutting Angle

data fails to show a distinct advantage.

Finally, various cuts have been performed by a tele-operated joystick under human control. Most of the cutting processes are successfully accomplished without any severe chattering. However, its measurement is not included in this paper due to space. Experimentally, the contact velocity is one of critical factors which initiates chattering.

6. CONCLUSIONS

Taking advantage of the passive compliance of the flexible manipulator, certain applications such as cutting a workpiece are performed with pure position control. This provides a simple, inexpensive solution for certain applications that otherwise could not be achieved with position control alone.

Both computer-controlled cutting and human-operated cutting were performed with minor chattering. However, contact velocity should remain very small to reduce chattering.

The contact with the workpiece causes a shift of the first natural frequency of a flexible arm due to the change of the boundary conditions. Different cutting angles produce different frequencies of vibrations due to the different compliances in the

direction of forcing.

Analytical studies predict 120 degrees cutting as the most desirable. However, this experimental investigation could not show distinct differences in the magnitude of chattering, although we may say that the 90 degree cutting angle generates a smaller magnitude of chattering in the Y direction. The compliance ellipsoid for our test bed is not elongated enough to make distinct differences in compliance. A different configuration could have made a more elongated ellipsoid, but further experimental tests have not been conducted due to physically limited location of the workpiece.

REFERENCES

[1] J. Craig, "Introduction to Robotics, Mechanics and Control", Addison-Wesley Publishing Co., 1989

5

[2] M. Spong and M.Vidyasagar, *"Robot Dynamics and Control"*, John Wiley and Sons, 1989

[3] F. Koeningsberger and J. Tlusty, *"Machine Tool Structures"*, Volume 1, Pergamon Press, 1970

[4] J. Peter, R. Snoeys and A. Decneut, *"The Proper Selection of Grinding Conditions in Cylinderical Plunge Grinding"*, Proceedings of the 16th Internal Machine Tool Design and Research Conference,

[5] Y. Liao and L. Shiang, *"Computer Simulation of Self-Exicited and Forced Vibrations in the External Cylinderical Plunge Grinding Proccess"*, The Winter Annual Meeting of ASME, San Francisco, CA, Dec 10-15,1989

[6] A. Shunsheruddin and S. Kim, *"Adaptive Control of the Cylinderical Plunge Grinding Process"*,

[7] R. Hahn and R. Linsay, *"Principles of Grinding..part1 Basic Relation-ships in Precision Grinding'*, Machinery, July-November 1971

[8] S. Kalpakjian, *"Manufacturing Processes for Engeering Materials"*, Addison- Wesley Publishing Co., 1984

[9] J. Lee, *"Dynamic Analysis and Control of Lightweight Manipulators with Flexible Parallel Link Mechanisms"*, Ph.D Thesis, School of Mechanical Engineering, Georgia Institute of Technology, 1990

[10] W. Book, *" Recursive Lagrangian Dynamics of Flexible Manipulators"*, International Journal of Robotics Research, Vol. 3 No.3, 1984

[11] K. Oosting and S.Dickerson, *"Simulation of a High-Speed Lightweight Arm"*, In Proceeding of the 1988 International Conference on Robotics and Automation,Vol.1,1988